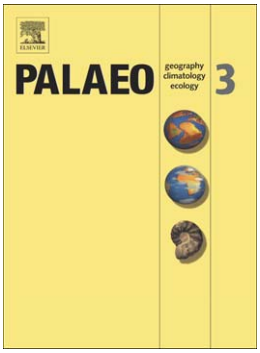

Arabia-Eurasia collision and the forcing of mid Cenozoic global cooling

Mark B. Allen, Howard A. Armstrong

PII: S0031-0182(08)00264-2
DOI: doi: 10.1016/j.palaeo.2008.04.021
Reference: PALAEO 4714

To appear in: *Palaeogeography*

Received date: 22 August 2007
Revised date: 11 March 2008
Accepted date: 15 April 2008

Please cite this article as: Allen, Mark B., Armstrong, Howard A., Arabia-Eurasia collision and the forcing of mid Cenozoic global cooling, *Palaeogeography* (2008), doi: 10.1016/j.palaeo.2008.04.021

Arabia-Eurasia collision and the forcing of mid Cenozoic global cooling

Mark B. Allen* and Howard A. Armstrong

Department of Earth Sciences, Durham University, Durham, DH1 3LE, UK

* m.b.allen@durham.ac.uk

Abstract

The end of the Eocene greenhouse world was the most dramatic phase in the long-term cooling trend of the Cenozoic Era. Here we show that the Arabia-Eurasia collision and the closure of the Tethys ocean gateway began in the Late Eocene at ~35 Ma, up to 25 million years earlier than in many reconstructions. We suggest that global cooling was forced by processes associated with the initial collision that reduced atmospheric CO_2. These are: 1) waning volcanism across southwest Asia; 2) increased organic carbon storage in Paratethyan basins (e.g. Black Sea and South Caspian); 3) increased silicate weathering in the collision zone and, 4) a shift towards modern patterns of ocean currents, associated with increased vigour in circulation and organic productivity.

Keywords: Eocene; Oligocene; Tethys; Arabia-Eurasia collision; global cooling.

1. Introduction

Stable isotopic data for the early Cenozoic (Paleocene to Eocene) show a long-term pattern of cooling (Miller et al., 1987; Zachos et al., 2001; Tripati et al., 2003) followed by the rapid expansion of the Antarctic continental ice sheet in the latest Eocene to earliest Oligocene (Ditchfield et al., 1994; Zachos et al., 2001). The latter

event, Oi-1, represents a 400 kyr-long glacial, initiated by reorganisation of the ocean/climate system. This is evidenced by global shifts in the distribution of marine biogenic sediments, including a ~1 km deepening of the calcite compensation depth (CCD) (Coxall et al., 2005) and an overall increase in ocean fertility (Baldauf and Barron, 1990; Salamy and Zachos, 1999; Thomas et al., 2000). A sharp positive carbon isotope excursion (~0.5 ‰) indicates a significant perturbation in the global carbon cycle (Zachos et al., 2001). High deep sea $\delta^{18}O$ values (~2.5 ‰) during this event indicate permanent ice sheets, ~50% the size of the present day Antarctica ice sheet (Zachos et al., 2001). Significant cool-water upwelling during Oi-1 (Kennett and Barker, 1990; Barron et al., 1991; Diester-Haass, 1996; Salamy and Zachos, 1999; Exon et al., 2002) is supported by a pattern of declining biotic diversity among marine micro-invertebrates and dinoflagellates (Cifelli, 1969; Corliss, 1979; Benson et al., 1984), diversification of the diatoms (Katz et al., 2004) and a widespread change from carbonate (calcareous nannoplankton, foraminifers) to biosiliceous (diatom) oozes along the Antarctic margin. Oi-1 also coincides with a shift in continental floral belts (Frakes et al., 1992) and aridification and cooling in continental interiors Dupont-Nivet et al., 2007; Zanazzi et al., 2007).

The causes of the Oi-1 glaciation remain contentious and have hitherto focused on drivers from the southern high latitudes. Two first order causal hypotheses dominate thinking on mid Cenozoic climate change: 1) opening of ocean gateways separating Antarctica from other continents (Kennett, 1977); 2) reduction of atmospheric CO_2 levels (DeConto and Pollard, 2003). Both hypotheses have caveats. Recent models indicate that changes in oceanic heat transport as the result of Antarctic isolation were too small to initiate Antarctic glaciation (Huber and Nof, 2006). Also, the precise timing of circum-Antarctic gateways is controversial (Pfuhl

and McCave, 2005; Scher and Martin, 2006: Livermore et al., 2007). End Eocene decline in atmospheric CO_2 is supported by proxy data (Pagani et al., 2005), but this leads to the question: what caused the decline?

Different lines of evidence indicates that initial collision of the Arabian and Eurasian plates and closure of the Tethys Ocean took place at ~35 Ma (Late Eocene), up to 25 million years earlier than in many plate tectonic or oceanographic reconstructions (Woodruff and Savin, 1989; McQuarrie et al., 2003; Guest et al., 2006), but consistent with geologic data from across the collision zone, used in other reconstructions to argue for an Eocene age (Hempton, 1985; Vincent et al., 2005; Jassim and Goff, 2006). This collision caused constriction of the Tethys Gateway, which previously linked the Indian and Atlantic oceans (Fig. 1). We hypothesize that this event caused large-scale, multiple feedbacks in the carbon cycle that promoted global cooling and the Oi-1 glaciation.

2. Date of initial Arabia-Eurasia continental collision

There is considerable evidence for a Late Eocene (~35 Ma) age for the initial Arabia-Eurasia collision and elimination of intervening Tethyan oceanic crust (Figs 2 and 3). Data include the timing of the following: compressional deformation, major surface uplift, exhumation, non-deposition or angular unconformities; sediment provenance switches and onset of terrestrial sedimentation, changes in palaeobiogeography and the switch-off of arc magmatism. The data divide into geographical sets on either side of the original plate suture; key regions are summarised in Fig. 3. Note that Arabia was a promontory of the African plate before the opening of the Red Sea in the mid Cenozoic, after initial Arabia-Eurasia collision.

To the south of the Arabia-Eurasia suture zone much of the collision history is recorded in the tectono-stratigraphy of the Zagros Mountains in SW Iran and adjacent parts of Iraq and Turkey. A regional Late Eocene – Early Oligocene angular unconformity is recognised in the northeast of the Zagros (Hessami et al., 2001) (Fig. 3), interpreted by these authors as the early record of collision in an incipient foreland basin. Over much of the Zagros, Oligocene deposition was dominated by shallow marine carbonates of the Asmari Formation and its equivalents (Nadjafi et al., 2004), but approaching the suture to the northeast the carbonates are replaced by sandstones of the Razak Formation, shed from the region of the suture zone (Beydoun et al., 1992). Close to the suture in southwest Iran, in the Kermanshah-Hamedan area, some of the thrusts in the Zagros are post-Late Eocene to pre-Early Miocene, and are unconformably overlain by Upper Oligocene – Lower Miocene conglomerates (Agard et al., 2005) (Fig. 3). The thrust stack contains both Eocene volcanics and sedimentary rocks of Eurasian affinity and Cretaceous sediments and ophiolites from the northeast side of the Arabian plate (Agard et al., 2005).

In northeast Iraq, Upper Eocene terrestrial clastics of the Gercus Formation unconformably overlie deformed Mesozoic strata (Dhannoun et al., 1988). These strata and their underlying unconformity indicate compressional deformation and at least local sub-aerial uplift and erosion of the northeast edge of the Arabian plate by the Late Eocene, and have been interpreted as indicators of initial continental collision at this time (Jassim and Goff, 2006).

At the eastern end of the collision zone in northern Oman, a record of stable carbonate sedimentation from the latest Cretaceous – early Tertiary was terminated by Late Oligocene – Miocene folding (Searle, 1988). Collectively, these data record compressional deformation on the north Arabian margin from the Late Eocene

onwards (Fig. 3). Late Eocene compressional deformation also occurred at the western side of the collision zone, from Syria at least as far west as Algeria (Guiraud and Bosworth, 1999; Benaouali-Mebarek et al., 2006); it is not clear where effects of the Arabia-Eurasia collision pass westwards in to the rather enigmatic "Atlas" phase of deformation on the North African margin.

North of the suture, the Eurasian plate preserves a similar record of Late Eocene – Oligocene compressional deformation, uplift and associated sedimentation (Fig. 2). Close to the suture zone (Fig. 2), strata and igneous rocks as young as the Middle Eocene were folded and thrust, in places onto the Arabian plate, before being unconformably overlain by Oligocene sediments (Hempton, 1985; Yilmaz, 1993; Yigitbas and Yilmaz, 1996; Agard et al., 2005). Late Eocene thrusting in the Kyrenia Range of northern Cyprus is documented by deformed flysch and olistostrome deposits of this age, overlain unconformably by Lower Oligocene conglomerates and turbidites (Robertson and Woodcock, 1986). In the Berit region of southeast Turkey, a mid Eocene to earliest Miocene melange incorporates material derived from the Eurasian margin and is overlain by Lower Miocene turbidites, indicating that the Arabian plate had underthrust Eurasia by the earliest Miocene (Robertson et al., 2004) (Fig. 3). Within south-central Turkey several sedimentary basins, including Ulukişla (Fig. 2), underwent Late Eocene compressional deformation, with folding, thrusting and exhumation of volcanic rocks, turbidites and other sedimentary rocks deposited during Paleocene – Middle Eocene extension (Clark and Robertson, 2005; Jaffey and Robertson, 2005) (Fig. 3).

Eocene strata in the NW Greater Caucasus were deformed, exhumed and eroded before the deposition of Oligocene clastics (Aleksin and Ratner, 1967) indicating at least local deformation in this region near to the Eocene-Oligocene

boundary (Fig. 3). Parts of the western Greater Caucasus were emergent by at least the Early Oligocene (Vincent et al., 2007). Upper Eocene olistostromes south of the Greater Caucasus are interpreted as the result of compressional deformation (Banks et al., 1997), while seismic data from the margins of the eastern Black Sea show compressional deformation in the Late Eocene (Robinson et al., 1996). Syn-sedimentary slumps accompanied deposition of Upper Eocene turbidites in the Talysh, at the western margin of the South Caspian Basin (Vincent et al., 2005) (Fig. 3). These relatively fine-grained marine strata are overlain by a coarsening-upwards Oligocene succession that includes boulder-scale conglomerates. This volcanic-free stratigraphy superseded a pre-late Eocene deep marine succession with abundant volcanism, including pillow basalts and tuffs. The Alborz range of northern Iran switched from a Middle Eocene depocentre, including turbidites and tuffs, into an emergent range by the early Oligocene (Stöcklin, 1974; Annell et al., 1975; Alavi,1996; Guest et al., 2006,) (Fig. 3). Late Eocene – Oligocene deformation therefore occurred far to the north of the suture, suggesting that deformation propagated rapidly into the interior of Eurasia at the time of initial plate collision (Figs 2 and 3) (Robinson et al., 1996; Banks et al., 1997; Vincent et al., 2005; Vincent et al., 2007).

A Late Eocene initial collision is consistent with faunal data. There was progressive creation of separate Mediterranean and Indian Ocean marine realms, and migration of Eurasian and African/Arabian non-marine faunas (Harzhauser et al., 2002; Kappelman et al., 2003; Harzhauser et al., 2007). This is demonstrated by the tridacnine and strombid bivalves (Harzhauser et al., 2007), which show biogeographical divergence in the Oligocene. Gastropod assemblages also define two separate Tethys sub-provinces during the Oligocene, with an ill-defined boundary

within Iran and a rapid increase in endemism in the early Miocene (Harzhauser et al., 2002). The influx of Eurasian mammals into Africa indicates a land connection between Africa-Arabia and Eurasia existed by the Oligocene-Miocene boundary (Kappelman et al., 2003).

Tethyan sections at the Eocene-Oligocene transition show coeval faunal overturn in benthic foraminifera, accompanied by decreasing ventilation, preceding an increased intensity of abyssal circulation associated with the initial entry of bottom waters (likely to be North Atlantic Deep Water, NADW) and bolivinid/uvigerinid planktonic foraminifera blooms along the northern Tethys margin (Barbieri et al., 2003).

3. Collision, the carbon cycle and oceanography

Late Eocene closure of Tethys was coincident with declining pCO_2 levels (Pagani et al., 2005), implicated as a major driver for global cooling and Antarctic glaciation (DeConto and Pollard, 2003). We propose four potential mechanisms for reducing pCO_2 associated with initial Arabia-Eurasia collision and its effects on carbon fluxes and/or oceanographic circulation: decline of arc magmatism; storage of organic carbon in sedimentary basins; increased silicate weathering; stimulation of more vigorous, meridional ocean currents.

3.1. Declining Eocene arc magmatism in southwest Eurasia.

Before the Arabia-Eurasia collision the Eurasian continental margin experienced arc magmatism as the result of the northwards subduction of Tethyan (strictly, Neo-Tethyan) oceanic crust. This magmatism provides a time constraint on the maximum likely age for initial continental collision, and would have been a net

source of atmospheric CO_2. Across much of Iran and Turkey and adjacent areas there was a highly productive magmatic arc/back-arc system between ~50 and ~35 Ma. Magmatism was coincident with the renewal of northern motion of Africa-Arabia with respect to Eurasia, after a hiatus between 75 and 49 Ma (Dewey et al., 1989). Peak magmatism occurred in the Middle Eocene, close to 40 Ma, at which time volcanic successions accumulated at a rate of ~1.8 mm/yr, reached 4-8 km in thickness and occurred across an area of >2 million km^2 (Amidi et al., 1984; Kazmin et al., 1986; Brunet et al., 2003; McQuarrie et al., 2003; Ramezani and Tucker, 2003; Alpaslan et al., 2004; Vincent et al., 2005; Arslan and Aslan, 2006; Fig. 4). In detail, at least 4 km of intermediate-acidic volcanics are intercalated with mid-Eocene Nummulitic limestones in the Urumieh-Dokhtar arc in Iran (Berberian et al., 1982). Eight kilometres of mainly Middle Eocene volcanics and volcanigenic turbidites are recorded from the Talysh, adjacent to the South Caspian Basin (Vincent et al., 2005). Five km of Eocene andesitic volcanics and deep water clastics were deposited in the Alborz Mountains (Stöcklin, 1974; Alavi, 1996). Volcanism waned in the Late Eocene and there was little activity in the Oligocene (Fig. 4), though minor and sporadic magmatism has continued to the present day over much of the collision zone (Pearce et al., 1990).

Declining arc magmatism in the Late Eocene is consisitent with the early deformation history of the collision zone (Fig. 2), whereby Late Eocene initial collision of the Arabian and Eurasian plates terminated oceanic subduction, ended back-arc continental extension across southwest Asia (Vincent et al., 2005) and generated compressional deformation and surface uplift. Abundant Middle Eocene arc magmatism across SW Asia would have promoted high atmospheric CO_2 levels, although the precise amount is not known. This highly productive arc coincides with

the Middle Eocene climatic optimum, previously attributed to an unspecified rise in ridge or arc magmatism (Bohaty and Zachos, 2003). Conversely, the sharp reduction in arc magmatism, brought about by initial Arabia-Eurasia collision, would have reduced CO_2 degassing into the atmosphere, and so acted to reduce global temperatures.

3.2. Isolation of Paratethys and organic carbon storage.

A new oceanographic configuration formed between the Alps and the Aral Sea during the Late Eocene and Oligocene (Veto, 1987; Jones and Simmons, 1997; Rögl, 1999; Fig. 4). The basins were isolated from the global circulation, were prone to anoxia, and are collectively referred to as Paratethys or the Paratethyan basins. In the South Caspian and Black Sea basins the depocentres were located over blocks of highly attenuated continental crust or even oceanic crust (Finetti et al., 1988; Mangino and Priestley, 1998). These basement blocks are products of Mesozoic or early Cenozoic extension across southwestern Asia. Upper Eocene and Oligocene strata are commonly mud-prone and organic-rich across the region (Robinson et al., 1996; Vincent et al., 2005). Such organic-rich mudrocks are the main hydrocarbon source rock for the prolific oil fields of the Carpathians and South Caspian Basin, and are the main potential source rock in the eastern Black Sea. Total organic carbon (TOC) values reach 14% for the 2000 m thick Maykop Suite in the South Caspian Basin (Robinson et al., 1996; Katz et al., 2000). In the ~1000 m thick coeval strata of the Greater Caucasus, estimated average TOC values are ~1.5 to 2%. Typical thicknesses for the age equivalent Menilite Formation in eastern Europe are ~300 m, with average TOC of 2% (Veto, 1987). Based on these estimates of stratal thicknesses, extents and

224 average TOC, we estimate total organic sedimentary carbon in the combined Maykop
225 and Menilite units at 60 x 10^{12} T.

226 Our estimate for organic carbon stored in the uppermost Eocene-Oligocene
227 strata of the Paratethyan basins corresponds to an average deposition rate of ~6 x 10^{12}
228 T per Ma through this interval, equivalent to ~12% of the estimated global organic
229 carbon flux in the late Paleogene (Raymo, 1994). This flux is a crude estimate, given
230 that the distribution of organic carbon within the succession is poorly known but
231 unlikely to be even. The overall effect of the carbon drawdown would have
232 suppressed atmospheric CO_2 levels throughout the latest Eocene and Oligocene.
233
234 *3.3. Increased silicate weathering.*
235 Continental collision and increased sub-aerial erosion in newly elevated areas
236 would enhance low latitude silicate weathering (Raymo and Ruddiman, 1992), which
237 in turn promotes CO_2 drawdown from the atmosphere by reactions that can be
238 summarised as:
239
240 $CO_2 + CaSiO_3 \rightarrow CaCO_3 + SiO_2$
241
242 Evidence for exposure and increased erosion comes from the presence of non-
243 marine clastics or uplifted areas across large parts of the Arabia-Eurasia collision zone
244 from the Late Eocene onwards. The precise contribution to global CO_2 drawdown
245 from silicate weathering in the collision zone is difficult to quantify, and likely to
246 have been small given the area and likely rates involved when compared with global
247 rates, but it acted in the right sense to promote climatic cooling. Enhanced weathering

and erosion could also help account for the increase in the oceanic $^{87}Sr/^{86}Sr$ in the Late Eocene (Richter et al., 1992; Mead and Hodell, 1995).

3.4. Oceanographic changes.

Closure of Tethys resulted in a restructuring of Indian and Atlantic Ocean currents, closer to a modern pattern of ocean circulation and upwelling (Fig. 1). In the Cretaceous to Eocene (the "Proteus Ocean" of Kennett and Barker, 1990) low latitude surface currents were dominated by the circum-global westwards flow from the Indian Ocean to the Pacific via the Tethys and Panama gateways (Bush, 1997; Hallam, 1969; Huber and Sloan, 2001; Fig. 1). At about 37.5 Ma circum-equatorial surface water was directed southwards in the Indian Ocean via the Agulhas Current, as a result of the constricting Tethys Gateway (Diekmann et al., 2004). This current is a possible source of the moisture thought to be a critical element in maintaining a large mid Cenozoic Antarctic ice sheet (Zachos et al., 2001). Within the western Tethys (Mediterranean) region there was an increased intensity of abyssal circulation associated with the initial entry of NADW across the Eocene-Oligocene transition (Barbieri et al., 2003). Influx of cold corrosive deep water at ~34 Ma was a likely cause of marked faunal overturn in benthic foraminifera (Coccioni and Galeotti, 2003). Contourite deposition began in Cyprus at ~36 Ma (Kahler and Stow, 1998), also indicating increased ocean current vigour.

Stable and Nd isotope data show that a marine connection between the Indian and Atlantic oceans persisted into the Miocene (Woodruff and Savin, 1989; Stille et al., 1996), but as argued here, this seaway cannot have been floored by oceanic crust.

Tethys closure was just one aspect of mid Cenozoic plate re-configuration and oceanographic change. The widening North Atlantic led to the start of NADW at ~35

Ma (Wold, 1994; Zachos et al., 2001; Via and Thomas, 2006). Atlantic circulation patterns similar to the present day were established at this time (Via and Thomas, 2006). Although the precise timing for the opening of Antarctic gateways is still debated, the trend towards isolation is clear in plate reconstructions (Livermore et al., 2007). Likewise, Mediterranean tectonics involved rapid compressional and extensional events in the early Cenozoic, in the context of the overall convergence of Africa and Europe (Dewey et al., 1989; Rubatto et al., 1998), but without complete severance of the Tethyan seaway west of Arabia.

Oceanographic changes have been implicated in global climate change via increased upwelling, organic productivity and hence atmospheric CO_2 drawdown (Diester-Haass and Zahn, 1996, 2001; Schumacher and Lazarus, 2004; Anderson and Delaney, 2005). Our point is that Late Eocene Tethys closure is a previously unappreciated factor in this global re-organisation.

4. Conclusions

Oceanographic, plate tectonic and climatic modelling studies commonly take ~14 to 10 Ma (mid Miocene) as both the end of the Tethys connection between the Indian and Atlantic oceans and the initial Arabia-Eurasia collision (Woodruff and Savin, 1989; McQuarrie et al., 2003). Our interpretation of the collision is that the last oceanic plate separation between Arabia and Eurasia was in the Late Eocene at ~35 Ma (Fig. 1), agreeing with previous estimates for this age based on geological patterns within the collision zone (Jassim and Goff, 2006; Vincent et al., 2007).

Initial Arabia-Eurasia plate collision and closure of the Tethys Ocean provides four complementary mechanisms for reducing atmospheric CO_2 and global cooling: 1) the waning of pre-collision arc magmatism, 2) storage of organic carbon in the

Paratethyan basins, 3) an increase in silicate weathering, 4) re-organisation of ocean currents, consistent with global end Eocene increases in ocean current vigour, organic productivity and hence CO_2 drawdown. We contend that all these mechanisms acted together to help take the Earth across a threshold into the icehouse world at the Oi-1 event.

Acknowledgements

We thank Steve Vincent, Mike Simmons, Howie Scher, James Baldini and Glenn Milne for discussions. Laurent Jolivet and Eduardo Garzanti provided helpful reviews. Supported by Durham University research project R050451.

Figures

Fig. 1. Palaeogeographic and oceanographic reconstructions before and after the demise of the Tethys Ocean gateway. (**A**) Eocene period, with westerly transport of warm Indian Ocean water into the Atlantic via Tethys. (**B**) Oligocene, with connection between the Indian and Atlantic oceans impeded by the Arabia-Eurasia collision zone. Ocean currents derived from Bush (1997); Diekmann et al. (2004); Kennett and Barker (1990); Stille et al. (1996); Thomas et al. (2003); Via and Thomas (2006); von der Heydt and Dijkstra (2006).

Fig. 2. Present topography of the Arabia-Eurasia collision, location map for regions summarised in Fig. 3, and position of the Arabia-Eurasia suture.

Fig. 3. Summary tectonostratigraphy for localities showing Late Eocene – Oligocene deformation and/or uplift. Localities shown on Fig. 2. Derived from: Stöcklin, (1974);

Annells et al., (1975); Searle, (1988); Banks et al., (1997); Beydoun et al., (1992); Hessami et al., (2001); Agard et al., (2005); Clark and Robertson, (2005); Vincent et al., (2005, 2007); Guest et al., (2006); Boulton and Robertson, (2006); Jassim and Goff, (2006); Robertson et al., (2006).

Fig. 4. Comparison of the present distribution of (A) Eocene and (B) Oligocene magmatic rocks across southwest Asia. Derived from principally from Emami et al., (1993); Şenel (2002). Other sources summarised in Vincent et al. (2005). (B) also shows the extent of Oligocene sediments from the Paratethyan basins (Veto, 1987).

References

Agard, P., Omrani, J., Jolivet, L., Mouthereau, F., 2005. Convergence history across Zagros (Iran): constraints from collisional and earlier deformation. International Journal of Earth Sciences 94, 401-419.

Alavi, M., 1996. Tectonostratigraphic synthesis and structural style of the Alborz mountain system in northern Iran. Journal of Geodynamics 21, 1-33.

Aleksin, A.G., Ratner, V.Y., 1967. Oil and gas fields of the hydrocarbon basins of Russian SFSR, Ukrainian SSR and Kazakh SSR. Explanatory notes to the album, Nauchno-Issledovatel'skaya Laboratoriya Geologii Zarubezhnykh Stran, 215pp.

Alpaslan, M., Frei, R., Boztug, D., Kurt, M.A., Temel, A., 2004. Geochemical and Pb-Sr-Nd isotopic constraints indicating an enriched-mantle source for late Cretaceous to early Tertiary volcanism, Central Anatolia, Turkey. International Geology Review 46, 1022-1041.

347 Amidi, S.M., Emami, M.H., Michel, R., 1984. Alkaline character of Eocene
348 volcanism in the middle part of Central Iran and its geodynamic situation.
349 Geologische Rundschau 73, 917-932.
350 Anderson, L.D., Delaney, M.L., 2005. Middle Eocene to early Oligocene
351 paleoceanography from Agulhas Ridge, Southern Ocean (Ocean Drilling
352 Program Leg 177, Site 1090). Paleoceanography 20, Art. No. PA1013, doi
353 10.1029/2004PA001043.
354 Annells, R.N., Arthurton, R.S., Bazley, R.A., Davies, R.G., 1975. Explanatory text of
355 the Qazvin and Rasht Quadrangles Map, E3 and E4. Geological Survey of Iran
356 94pp.
357 Arslan, A., Aslan, Z., 2006. Mineralogy, petrography and whole-rock geochemistry of
358 the Tertiary granitic intrusions in the Eastern Pontides, Turkey. Journal of Asian
359 Earth Sciences 27, 177-193.
360 Baldauf, J.G. , Barron, J.A., 1990. Evolution of biosiliceous sedimentation patterns
361 Eocene through Quaternary: paleoceanographic response to polar cooling. In: U.
362 Bleil and J. Thiede (Editors), Geological history of the Polar Oceans: Arctic
363 versus Antarctic. Kluwer, Dordrecht, pp. 575-607.
364 Banks, C.J., Robinson, A.G., Williams, M.P., 1997. Structure and regional tectonics
365 of the Achara-Trialet fold belt and the adjacent Rioni and Kartli foreland basins,
366 republic of Georgia. In: A. Robinson (Editor), Regional and petroleum geology
367 of the Black Sea and surrounding region. AAPG Memoir 68 pp. 331-346.
368 Barbieri, R., Benjamini, C., Monechi, S., Reale, V., 2003. Stratigraphy and benthic
369 foraminiferal events across the Middle-Late Eocene transition in the Western
370 Negev., Israel. In: D.R. Prothero, L.C. Ivany and E.A. Nesbitt (Editors), From

greenhouse to icehouse: The marine Eocene-Oligocene transition. Columbia University Press, New York, pp. 453-471.

Barron, J.A., Baldauf, J.G., Barrera, E., Caulet, J.P., Huber, B.T., Keating, B.H., Lazarus, D., Sakai, H., Thierstein, H. R., Wei, W., 1991. Biochronologic and magnetochronologic synthesis of Leg 119 sediments fromthe Kerguelen Plateau and Pryz Bay, Antarctica. Proceedings of the Ocean Drilling Program, Scientific Results, 119, 813-847.

Benaouali-Mebarek, N., de Lamotte, D.F., Roca, E., Bracene, R., Faure, J.L., Sassi, W., Roure, F., 2006. Post-Cretaceous kinematics of the Atlas and Tell systems in central Algeria: Early foreland folding and subduction-related deformation. Comptes Rendus Geoscience 338, 115-125.

Benson, R.H., Chapman, R.E., Deck, L.T., 1984. Paleoceanographic events and deep-sea ostracodes. Science 224, 1334-1336.

Berberian, F., Muir, I.D., Pankhurst, R.J., Berberian, M., 1982. Late Cretaceous and early Miocene Andean-type plutonic activity in northern Makran and Central Iran. Journal of the Geological Society 139, 605-614.

Beydoun, Z.R., Hughes Clarke, M.W., Stoneley, R., 1992. Petroleum in the Zagros Basin: a late Tertiary foreland basin overprinted onto the outer edge of a vast hydrocarbon-rich Paleozoic-Mesozoic passive-margin shelf. In: R. MacQueen and D. Leckie (Editors), Foreland Basins and Foldbelts. AAPG Memoir 55, pp. 309-339.

Bohaty, S.M., Zachos, J.C., 2003. Significant Southern Ocean warming event in the late middle Eocene. Geology 31, 1017-1020.

Boulton, S.J., Robertson, A.H.F., 2006. Tectonic and sedimentary evolution of the Cenozoic Hatay Graben, Southern Turkey: a two-phase model for graben

evolution. In: A.H.F. Robertson and D. Mountrakis (Editors), Tectonic Development of the Eastern Mediterranean Region. Geological Society of London, Special Publications 260, London, pp. 613-634.

Brunet, M.F., Korotaev, M.V., Ershov, A.V., Nikishin, A.M., 2003. The South Caspian Basin: a review of its evolution from subsidence modelling. Sedimentary Geology 156, 119-148.

Bush, A.B.G., 1997. Numerical simulation of the Cretaceous Tethys circumglobal current. Science, 275 807-810.

Cifelli, R., 1969. Radiation of Cenozoic planktonic foraminifera. Systematic Zoology 18, 154-168.

Clark, M., Robertson, A., 2005. Uppermost Cretaceous-Lower Tertiary Ulukisla Basin, south- central Turkey: sedimentary evolution of part of a unified basin complex within an evolving Neotethyan suture zone. Sedimentary Geology 173, 15-51.

Coccioni, R., Galeotti, S., 2003. Deep-water benthic foraminiferal events from the Massignano Eocene/Oligocene boundary stratotype, central Italy. In: D.R. Prothero, L.C. Ivany and E.A. Nesbitt (Editors), From Greenhouse to Icehouse: The Marin Eocene - Oligocene transition. Columbia University Press, New York, pp. 438-453.

Corliss, B.H., 1979. Response of the deep sea benthic foraminifera to development of the psychrosphere near the Eocene-Oligocene boundary. Nature 282, 63-65.

Coxall, H.K., Wilson, P.A., Palike, H., Lear, C.H., Backman, J., 2005. Rapid stepwise onset of Antarctic glaciation and deeper calcite compensation in the Pacific Ocean. Nature 433, 53-57.

420 DeConto, R.M., Pollard, D., 2003. Rapid Cenozoic glaciation of Antarctica induced
421 by declining atmospheric CO_2. Nature 421, 245-249.
422 Dewey, J.F., Helman, M.L., Turco, E., Hutton, D.H.W., Knott, S.D., 1989.
423 Kinematics of the western Mediterranean. In: M.P. Coward, D. Dietrich and
424 R.G. Park (Editors), Alpine Tectonics. Special Publication of the Geological
425 Society, London, pp. 265-283.
426 Dhannoun, H.Y., Aldabbagh, S.M.A., Hasso, A.A., 1988. The Geochemistry of the
427 Gercus Red-Bed Formation of Northeast Iraq. Chemical Geology 69, 87-93.
428 Diekmann, B., Kuhn, G., Gersonde, R., Mackensen, A., 2004. Middle Eocene to early
429 Miocene environmental changes in the sub-Antarctic Southern Ocean: evidence
430 from biogenic and terrigenous depositional patterns at ODP Site 1090. Global
431 and Planetary Change 40, 295-313.
432 Diester-Haass, L., Zahn, R., 2001. Paleoproductivity increase at the Eocene-
433 Oligocene climatic transition: ODP/DSDP sites 763 and 592. Palaeogeography
434 Palaeoclimatology Palaeoecology 172, 153-170.
435 Diester-Haass, L., 1996. Late Eocene-Oligocene paleoceanography in the southern
436 Indian Ocean (ODP Site 744). Marine Geology 130, 99-119.
437 Diester-Haass, L., Zahn, R., 1996. Eocene-Oligocene transition in the Southern
438 Ocean: History of water mass circulation and biological productivity. Geology
439 24, 163-166.
440 Ditchfield, P.W., Marshall, J.D., Pirrie, D., 1994. High latitude palaeotemperature
441 variation: New data from the Tithonian to Eocene of James Ross Island,
442 Antarctica. Palaeogeography, Palaeoclimatology, Palaeoecology 107, 79-101.

443 Dupont-Nivet, G. Krijgsman, W., Langereis, C.G., Abels, H.A., Dai, S., Fang, X.M.,
444 2007. Tibetan plateau aridification linked to global cooling at the Eocene-
445 Oligocene transition. Nature 445, 635-638.
446 Emami, M.H., Sadeghi, M.M.M., Omrani, S.J., 1993. Magmatic map of Iran.
447 Geological Survey of Iran, Tehran.
448 Exon, N.F. and 28 others, 2002. Drilling reveals climatic consequences of Tasmanian
449 gateway opening. Eos, Transactions American Geophysical Union 83, 253-259.
450 Frakes, L.A., Francis, J.E. , Sykes, J.I., 1992. Climate Modes of the Phanerozoic.
451 Cambridge University Press, Cambridge, 274 pp.
452 Finetti, I., Bricchi, G., Del Ben, A., Pipan, M., Xuan, Z., 1988, Geophysical study of
453 the Black Sea. Bolletino di Geofisica Teorica ed Applicata 30, 197-324.
454 Guest, B., Stockli, D.F., Grove, M., Axen, G.J., Lam, P.S., Hassanzadeh, J., 2006.
455 Thermal histories from the central Alborz Mountains, northern Iran:
456 Implications for the spatial and temporal distribution of deformation in northern
457 Iran. Geological Society of America Bulletin 118, 1507-1521.
458 Guiraud, R., Bosworth, W., 1999. Phanerozoic geodynamic evolution of northeastern
459 Africa and the northwestern Arabian platform. Tectonophysics 315, 73-108.
460 Hallam, A., 1969. Faunal realms and facies in the Jurassic. Palaeontology 12, 1-18.
461 Harzhauser, M., Piller, W.E., Steininger, F.F., 2002. Circum-Mediterranean Oligo-
462 Miocene biogeographic evolution - the gastropods' point of view.
463 Palaeogeography Palaeoclimatology Palaeoecology 183, 103-133.
464 Harzhauser, M., Kroh, A., Mandic, O., Piller, W.E., Gohlich, U., Reuter, M., Berning,
465 B., 2007, Biogeographic responses to geodynamics: A key study all around the
466 Oligo-Miocene Tethyan Seaway. Zoologischer Anzeiger 246, 241-256.

467 Hempton, M.R., 1985. Structure and deformation history of the Bitlis suture near
468 Lake Hazar, southeastern Turkey. Geological Society of America Bulletin 96,
469 233-243.
470 Hessami, K., Koyi, H.A., Talbot, C.J., Tabasi, H., Shabanian, E., 2001. Progressive
471 unconformities within an evolving foreland fold-thrust belt, Zagros Mountains.
472 Journal of the Geological Society, London 158, 969-981.
473 Huber, B.T., Sloan, L.C., 2001. Heat transport, deep waters, and thermal gradients:
474 coupled simulation of an Eocene greenhouse climate. Geophysical Research
475 Letters 28, 3481-3484.
476 Huber, M., Nof, D., 2006. The ocean circulation in the southern hemisphere and its
477 climatic impacts in the Eocene. Palaeogeography Palaeoclimatology
478 Palaeoecology 231, 9-28.
479 Jaffey, N., Robertson, A., 2005. Non-marine sedimentation associated with
480 Oligocene-Recent exhumation and uplift of the central Taurus Mountains, S
481 Turkey. Sedimentary Geology 73, 53-89.
482 Jassim, S.Z., Goff, J.C., 2006. Phanerozoic development of the northern Arabian
483 Plate. In: S.Z. Jassim and J.C. Goff (Editors), Geology of Iraq. Dolin, Prague,
484 pp. 32-44.
485 Jones, R.W., Simmons, M.D., 1997. A review of the stratigraphy of Eastern
486 Paratethys (Oligocene-Holocene), with particular emphasis on the Black Sea. In:
487 A. Robinson (Editor), Regional and petroleum geology of the Black Sea and
488 surrounding region. AAPG Memoir 68, pp. 39-52.
489 Kahler, G., Stow, D.A.V., 1998. Turbidites and contourites of the Palaeogene Lefkara
490 Formation, southern Cyprus. Sedimentary Geology 115, 215-231.

491 Kappelman, J. and 21 others, 2003. Oligocene mammals from Ethiopia and faunal
492 exchange between Afro-Arabia and Eurasia. Nature 426, 549-552.
493 Katz, B., Richards, B., Long, D., Lawrence, W., 2000. A new look at the components
494 of the petroleum system of the South Caspian Basin. Journal of Petroleum
495 Science and Engineering, 28 161-182.
496 Katz, M.E., Finkel, Z.V., Grzebyk, D., Knoll, A.H., Falkowski, P.G., 2004.
497 Evolutionary trajectories and biogeochemical impacts of marine eukaryotic
498 phytoplankton. Annual Review of Ecology and Evolutionary Systematics 35,
499 523-556.
500 Kazmin, V.G. Sborshchikov, I.M., Ricou, L.-E., Zonenshain, L.P., Boulin, J.,
501 Knipper, A.L., 1986. Volcanic belts as markers of the Mesozoic-Cenozoic active
502 margin of Eurasia. Tectonophysics 123, 123-152.
503 Kennett, J.P., 1977. Cenozoic evolution of Antarctic glaciation, the circum-Antarctic
504 ocean and their impact on global paleoceanography. Journal of Geophysical
505 Research 82, 843-860.
506 Kennett, J.P., Barker, P.F., 1990. Latest Cretaceous to Cenozoic climate and
507 oceanographic developments in the Weddell Sea, Antarctica: an ocean drilling
508 perspective. Proceedings of the Ocean Drilling Program, Scientific Results 113,
509 937-960.
510 Livermore, R., Hillenbrand, C.D., Meredith, M., Eagles, G., 2007. Drake Passage and
511 Cenozoic climate: An open and shut case? Geochemistry Geophysics
512 Geosystems 8, art. no. Q01005, doi 10.1029/2005GC001224.
513 Mangino, S., Priestley, K., 1998, The crustal structure of the southern Caspian region.
514 Geophysical Journal International 133, 630-648.

McQuarrie, N., Stock, J.M., Verdel, C., Wernicke, B., 2003. Cenozoic evolution of Neotethys and implications for the causes of plate motions. Geophysical Research Letters 30: art. no. 2036 doi 10.1029/2003GL017992.

Mead, G.A., Hodell, D.A., 1995. Controls on the Sr-87/Sr-86 composition of seawater from the Middle Eocene to Oligocene - Hole 689B, Maud Rise, Antarctica. Paleoceanography 10, 327-346.

Miller, K.G., Fairbanks, R.A., Mountain, G.S., 1987. Tertiary oxygen isotope synthesis, sea-level history and continental margin erosion. Paleoceanography 2, 1-19.

Nadjafi, M., Mahboubi, A., Moussavi-Harami, R. , Mirzaee, R., 2004. Depositional history and sequence stratigraphy of outcropping Tertiary carbonates in the Jahrum and Asmari formations, Shiraz area (SW Iran). Journal of Petroleum Geology 27, 179-190.

Pagani, M., Zachos, J.C., Freeman, K.H., Tipple, B., Bohaty, S., 2005. Marked decline in atmospheric carbon dioxide concentrations during the Paleogene. Science 309, 600-603.

Pearce, J.A., Bender, J. F., Delong, S. E., Kidd, W. S. F., Low, P. J., Guner, Y., SaRöglu, F., Yilmaz, Y., Moorbath, S., Mitchell, J. G., 1990. Genesis of collision volcanism in eastern Anatolia, Turkey. Journal of Volcanology and Geothermal Research 44, 189-229.

Pfuhl, H.A., McCave, I.N., 2005. Evidence for late Oligocene establishment of the Antarctic Circumpolar Current. Earth and Planetary Science Letters 235, 715-728.

538 Ramezani, J., Tucker, R.D., 2003. The Saghand region, central Iran: U-Pb
539 geochronology, petrogenesis and implications for Gondwana tectonics.
540 American Journal of Science 303, 622-665.
541 Raymo, M.E., 1994. The Himalayas, organic-carbon burial, and climate in the
542 Miocene. Paleoceanography 9, 399-404.
543 Raymo, M.E., Ruddiman, W.F., 1992. Tectonic forcing of late Cenozoic climate.
544 Nature 359, 117-122.
545 Richter, F.M., Rowley, D.B., DePaolo, D.J., 1992. Sr isotope evolution of seawater -
546 the role of tectonics. Earth and Planetary Science Letters 109, 11-23.
547 Robertson, A., Unlugenc, O.C., Inan, N., Tasli, K., 2004. The Misis-Andirin complex:
548 a mid-tertiary melange related to late-stage subduction of the southern Neotethys
549 in S Turkey. Journal of Asian Earth Sciences 22, 413-453.
550 Robertson, A.H.F., Ustaomer, T., Parlak, O., Unlugenc, U. C., Tasli, K., Inan, N.,
551 2006. The Berit transect of the Tauride thrust belt, S Turkey: Late Cretaceous-
552 Early Cenozoic accretionary/collisional processes related to closure of the
553 Southern Neotethys. Journal of Asian Earth Sciences, 27, 108-145.
554 Robertson, A.H.F., Woodcock, N.H., 1986. The role of the Kyrenia Range lineament,
555 Cyprus, in the geological evolution of the eastern Mediterranean area.
556 Philosophical Transactions of the Royal Society of London Series A-
557 Mathematical Physical and Engineering Sciences 317, 141-177.
558 Robinson, A., Rudat, J., Banks, C., Wiles, R., 1996. Petroleum geology of the Black
559 Sea. Marine and Petroleum Geology 13, 195-223.
560 Rögl, F., 1999. Mediterranean and Paratethys. Facts and hypotheses of an Oligocene
561 to Miocene paleogeography (short overview). Geologica Carpathica 50, 339-
562 349.

563 Rubatto, D., Gebauer, D., Fanning, M., 1998, Jurassic formation and Eocene
564 subduction of the Zermatt-Saas-Fee ophiolites: implications for the geodynamic
565 evolution of the Central and Western Alps. Contributions to Mineralogy and
566 Petrology 132, 269-287.
567 Salamy, K.A., Zachos, J.C., 1999. Latest Eocene-early Oligocene climate change and
568 Southern Ocean fertility: Inferences from sediment accumulation and stable
569 isotope data. Palaeogeography Palaeoclimatology Palaeoecology 145, 61-77.
570 Scher, H.D., Martin, E.E., 2006. Timing and climatic consequences of the opening of
571 Drake Passage. Science 312, 428-430.
572 Schumacher, S., Lazarus, D., 2004. Regional differences in pelagic productivity in the
573 late Eocene to early Oligocene - a comparison lower of southern high latitudes
574 and longitudes. Palaeogeography Palaeoclimatology Palaeoecology 214, 243-
575 263.
576 Searle, M.P., 1988. Structure of the Musandam Culmination (Sultanate-Of-Oman And
577 United-Arab-Emirates) and the Straits of Hormuz Syntaxis. Journal of the
578 Geological Society 145, 831-845.
579 Şenel, M., 2002. Geological map of Turkey. General Directorate of Mineral Research
580 and Exploration, Ankara.
581 Stille, P., Steinmann, M., Riggs, S.R., 1996. Nd isotope evidence for the evolution of
582 the paleocurrents in the Atlantic and Tethys Oceans during the past 180 Ma.
583 Earth and Planetary Science Letters 144, 9-19.
584 Stöcklin, J., 1974. Northern Iran: Alborz mountains. In: A. Spencer (Editor),
585 Mesozoic-Cenozoic orogenic belts: data for orogenic studies. Special
586 Publication of the Geological Society of London, pp. 213-234.

587 Thomas, D.J., Bralower, T.J., Jones, C.E., 2003. Neodymium isotopic reconstruction
588 of late Paleocene-early Eocene thermohaline circulation. Earth and Planetary
589 Science Letters 209, 309-322.
590 Thomas, E., Zachos, J.C. , Bralower, T.J., 2000. Deep-sea environments on a warm
591 Earth: Latest Paleocene–early Eocene. In: B.T. Huber, K.G. MacLeod and S.L.
592 Wing (Editors), Warm Climates in Earth History. Cambridge University Press,
593 New York, pp. 132-160.
594 Tripati, A., Delaney, M.L., Zachos, J.C., Anderson, L.D., Kelly, D.C., Elderfield, H.,
595 2003. Tropical sea surface temperature reconstructions for the early Paleogene
596 using Mg/Ca ratios of planktonic foraminifera. Paleooceanography 18, art. no.
597 1011, doi 10.1029/2003PA000937.
598 Veto, I., 1987. An Oligocene sink for organic-carbon - upwelling in the Paratethys.
599 Palaeogeography Palaeoclimatology Palaeoecology 60, 143-153.
600 Via, R.K., Thomas, D.J., 2006. Evolution of Atlantic thermohaline circulation: Early
601 Oligocene onset of deep-water production in the North Atlantic. Geology 34,
602 441-444.
603 Vincent, S.J., Allen, M.B., Ismail-Zadeh, A.D., Flecker, R., Foland, K.A., Simmons,
604 M.D. 2005. Insights from the Talysh of Azerbaijan into the Paleogene evolution
605 of the South Caspian region. Bulletin of the Geological Society of America 117,
606 1513-1533.
607 Vincent, S.J., Morton, A.C., Carter, A., Gibbs, S., Barabadze, T.G., 2007. Oligocene
608 uplift of the Western Greater Caucasus: an effect of initial Arabia-Eurasia
609 collision. Terra Nova 19, 160-166.

610 von der Heydt, A., Dijkstra, H.A., 2006. Effect of ocean gateways on the global ocean
611 circulation in the late Oligocene and early Miocene. Paleoceanography 21, art.
612 no. PA1101 doi:10.1029/2005PA001149.
613 Wold, C.N., 1994. Cenozoic sediment accumulation on drifts in the northern North
614 Atlantic. Paleoceanography 9, 917-941.
615 Woodruff, F., Savin, S.M., 1989. Miocene deepwater oceanography.
616 Paleoceanography 4, 87-140.
617 Yigitbas, E., Yilmaz, Y., 1996. New evidence and solution to the Maden Complex
618 controversy of the Southeast Anatolian orogenic belt (Turkey). Geologische
619 Rundschau 85, 250-263.
620 Yilmaz, Y., 1993. New evidence and model on the evolution of the southeast
621 Anatolian orogen. Bulletin of the Geological Society of America 105, 251-271.
622 Zachos, J.C., Pagani, M., Sloan, E.T., Billups, K., 2001. Trends, rhythms, and
623 aberations in global climate 65 Ma to present. Science 292, 686-694.
624 Zanazzi, A., Kohn, M.J., MacFadden, B.J., Terry, D.O., 2007. Large temperature drop
625 across the Eocene-Oligocene transition in central North America. Nature 445,
626 639-642.

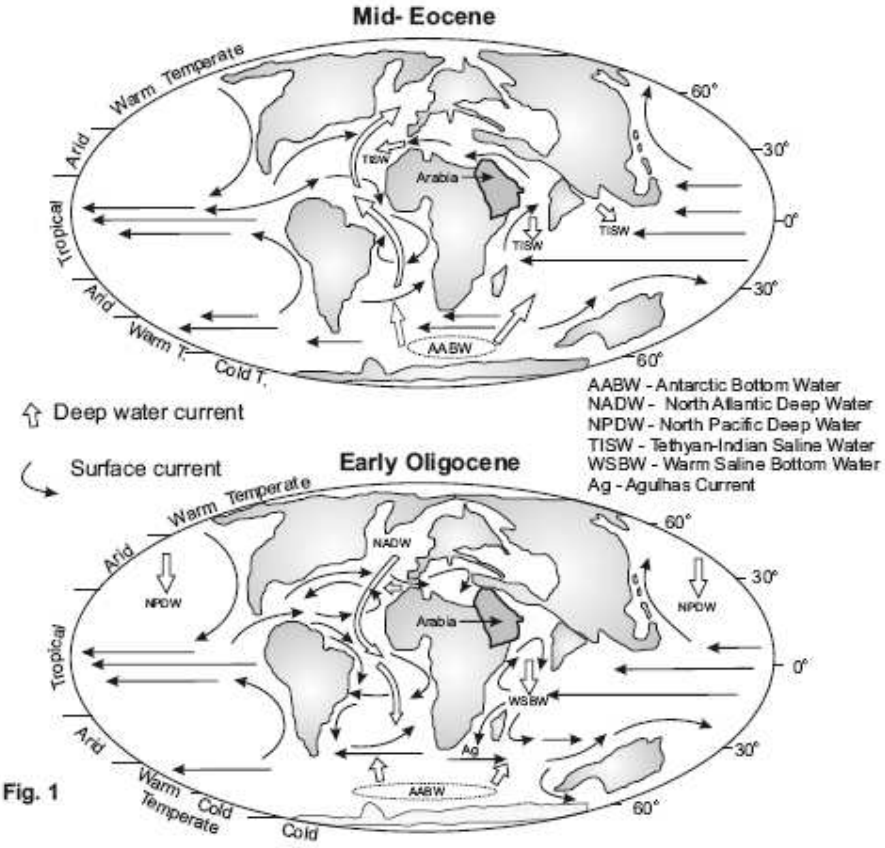

Fig. 1

627

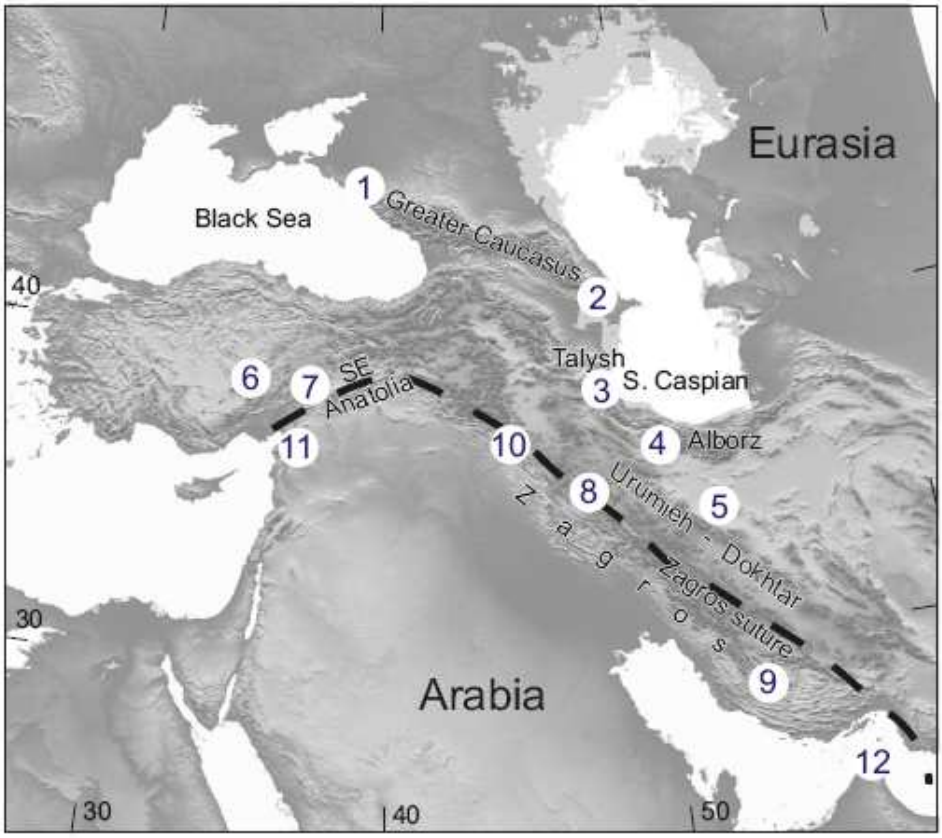

Fig. 2

628

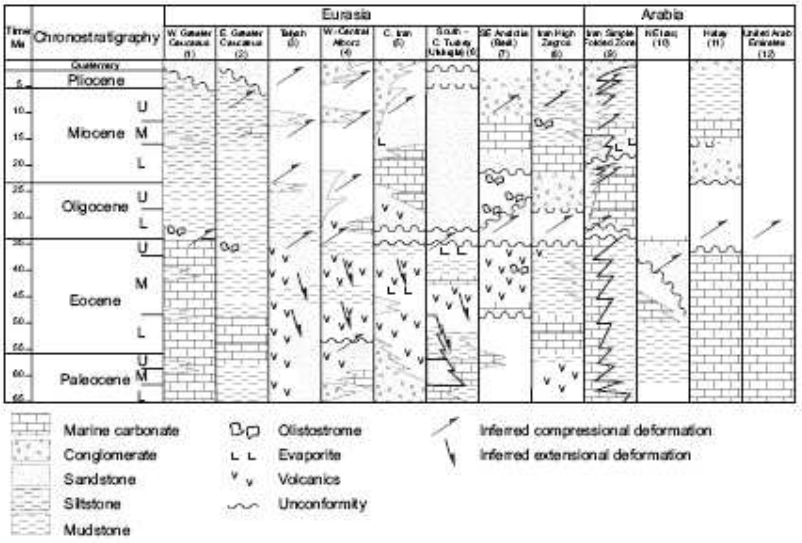

Fig. 3

629

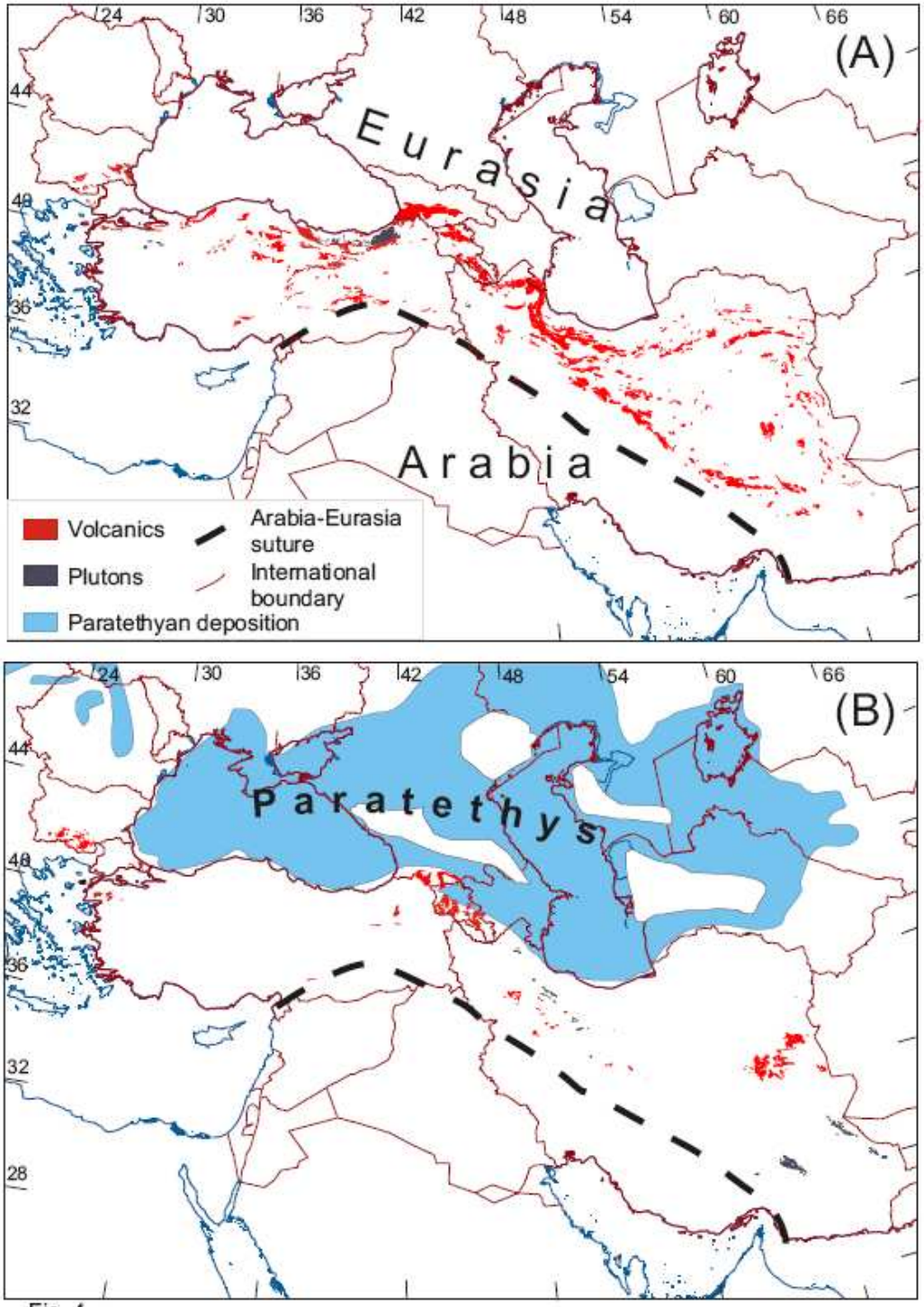

630 Fig. 4